Spectral dispersion modeling of virtually imaged phased array by using angular spectrum of plane waves

Xinrong Hu,[1,2,*] Qiang Sun,[1] Jing Li,[1,2] Chun Li,[1] Ying Liu,[1] and Jianzhong Zhang[1]

[1] *Changchun Institute of Optics, Fine Mechanics and Physics, Chinese Academy of Sciences, Changchun, Jilin, 130033, China*

[2] *Graduate School of the Chinese Academy of Sciences, Beijing, 100049, China*

[*] *huxr062768@mail.nwpu.edu.cn*

Abstract: We present an analytical treatment for the relatively new spectral disperser termed virtually imaged phased array (VIPA). Angular spectrum representation of the input Gaussian beam helps us obtain an exact analytic dispersion model and a dispersion law for a general VIPA by using the principle of multiple-beam interference. The consideration of the optical aberrations caused by refractions makes our model more accurate and practical than previous models. The validity of the proposed dispersion law has been validated theoretically by comparing with previous results. Some considerations of using a VIPA are also provided.

OCIS codes: (050.2230) Fabry-Perot; (050.1960) Diffraction theory; (260.3160) Interference; (070.4790) Spectrum analysis; (080.1010) Aberrations (global).

References and links

1. M. Shirasaki, "Large angular dispersion by a virtually imaged phased array and its application to a wavelength demultiplexer," Opt. Lett. **21**(5), 366–368 (1996).
2. M. Shirasaki, "Chromatic-dispersion compensator using virtually imaged phased array," IEEE Photon. Technol. Lett. **9**(12), 1598–1660 (1997).
3. M. Shirasaki, "Virtually imaged phased array," Fujitsu Sci. Tech. J. **35**(1), 113–125 (1999).
4. L. Garrett, A. Gnauck, M. Eiselt, R. Tkach, C. Yang, C. Mao, and S. Cao, "Demonstration of virtually-imaged phased-array device for tunable dispersion compensation in 16 times;10 Gb/s WDM transmission over 480 km standard fiber," in Optical Fiber Communication Conference, 2000 **4**, 187–189 (2000).
5. S. Xiao and A. M. Weiner, "2-D wavelength demultiplexer with potential for ≥ 1000 channels in the C-band," Opt. Express **12**(13), 2895–2902 (2004).
6. S. X. Wang, S. Xiao, and A. M. Weiner, "Broadband, high spectral resolution 2-D wavelength-parallel polarimeter for Dense WDM systems," Opt. Express **13**(23), 9374–9380 (2005).
7. G.-H. Lee, S. Xiao, and A. M. Weiner, "Optical dispersion compensator with >> 4000-ps/nm tuning range using a virtually imaged phased array (VIPA) and spatial light modulator (SLM)," IEEE Photon. Technol. Lett. **18**(17), 1819–1821 (2006).
8. S. Xiao, J. D. McKinney, and A. M. Weiner, "Photonic microwave arbitrary waveform generation using a VIPA direct space-to-time pulse shaper," IEEE Photon. Technol. Lett. **16**(8), 1936–1938 (2004).
9. S. T. Cundiff and A. M. Weiner, "Optical arbitrary waveform generation," Nat. Photonics **4**(11), 760–766 (2010).
10. V. R. Supradeepa, E. Hamidi, D. E. Leaird, and A. M. Weiner, "New aspects of temporal dispersion in high-resolution Fourier pulse shaping: a quantitative description with virtually imaged phased array pulse shapers," J. Opt. Soc. Am. B **27**(9), 1833–1844 (2010).
11. A. M. Weiner, "Ultrafast optical pulse shaping: a tutorial review," Opt. Commun. **284**(15), 3669–3692 (2011).
12. K. Goda, K. K. Tsia, and B. Jalali, "Serial time-encoded amplified imaging for real-time observation of fast dynamic phenomena," Nature **458**(7242), 1145–1149 (2009).
13. S. A. Diddams, L. Hollberg, and V. Mbele, "Molecular fingerprinting with the resolved modes of a femtosecond laser frequency comb," Nature **445**(7128), 627–630 (2007).
14. C. Wang, Z. Ding, S. Mei, H. Yu, W. Hong, Y. Yan, and W. Shen, "Ultralong-range phase imaging with orthogonal dispersive spectral-domain optical coherence tomography," Opt. Lett. **37**(21), 4555–4557 (2012).
15. W. Bao, Z. Ding, P. Li, Z. Chen, Y. Shen, and C. Wang, "Orthogonal dispersive spectral-domain optical coherence tomography," Opt. Express **22**(8), 10081–10090 (2014).

#217519 - $15.00 USD Received 21 Jul 2014; revised 29 Nov 2014; accepted 30 Nov 2014; published 5 Jan 2015

16. K. K. Tsia, K. Goda, D. Capewell, and B. Jalali, "Simultaneous mechanical-scan-free confocal microscopy and laser microsurgery," Opt. Lett. **34**(14), 2099–2101 (2009).
17. P. Metz, J. Adam, M. Gerken, and B. Jalali, "Compact, transmissive two-dimensional spatial disperser design with application in simultaneous endoscopic imaging and laser microsurgery," Appl. Opt. **53**(3), 376–382 (2014).
18. L. Yang, "Analytical treatment of virtual image phase array," in *Proceedings of Optical Fiber Communication Conference and Exhibit (OFC2002)*, pp. 321–322.
19. A. Vega, A. M. Weiner, and C. Lin, "Generalized grating equation for virtually-imaged phased-array spectral dispersers," Appl. Opt. **42**(20), 4152–4155 (2003).
20. S. Xiao, A. M. Weiner, and C. Lin, "A dispersion law for virtually imaged phased-array spectral dispersers based on paraxial wave theory," IEEE J. Quantum Electron. **40**(4), 420–426 (2004).
21. S. Xiao, "The spatial chirp effect and dispersion law of virtually imaged phased array (VIPA) wavelength demultiplexer," M. S. Thesis, Purdue University, August, 2003.
22. A. Mokhtari and A. A. Shishegar, "Rigorous vectorial Gaussian beam modeling of spectral dispersing performance of virtually imaged phased arrays," J. Opt. Soc. Am. B **26**(2), 272–278 (2009).
23. A. Mokhtari and A. A. Shishegar, "Rigorous 3D vectorial Gaussian beam modeling of demultiplexing performance of virtually-imaged-phased-arrays," Progress In Electromagnetics Research M **13**, 1–16 (2010).
24. D. J. Gauthier, "Comment on "Generalized grating equation for virtually imaged phased-array spectral dispersers"," Appl. Opt. **51**(34), 8184–8186 (2012).
25. A. M. Weiner, "Reply to Comment on "Generalized grating equation for virtually imaged phased-array spectral dispersers"," Appl. Opt. **51**(34), 8187–8189 (2012).
26. C. F. McMillan, N. L. Parker, and D. R. Goosman, "Efficiency enhancements for Fabry-Perots used in velocimetry," Appl. Opt. **28**(5), 826–827 (1989).
27. D. R. Goosman, "Formulas for Fabry-Perot velocimeter performance using both stripe and multifrequency techniques," Appl. Opt. **30**(27), 3907–3923 (1991).
28. M. Born and E. Wolf, *Principles of Optics: Electromagnetic Theory of Propagation, Interference and Diffraction of Light, 7nd ed.* (Cambridge University, 1999). pp. 313–386.
29. J. W. Goodman, *Introduction to Fourier Optics, 2nd ed.* (McGraw-Hill, 1996), pp. 54–72.
30. L. Novotny and B. Hecht, *Principles of Nano-Optics* (Cambridge University, 2006). pp. 38–56.
31. J. B. Keller, "Geometrical theory of diffraction," J. Opt. Soc. Am. **52**(2), 116–130 (1962).
32. P. Metz, H. Block, C. Behnke, M. Krantz, M. Gerken, and J. Adam, "Tunable elastomer-based virtually imaged phased array," Opt. Express **21**(3), 3324–3335 (2013).
33. S. Xiao, A. M. Weiner, and C. Lin, "Experimental and theoretical study of hyperfine WDM demultiplexer performance using the virtually imaged phased-array (VIPA)," J. Lightwave Technol. **23**(3), 1456–1467 (2005).

1. Introduction

The virtually imaged phased array (VIPA) is a multiple-beam interference spectral disperser that provides several advantages over the diffraction gratings, which includes large angular dispersion, low polarization sensitivity, simple structure and low cost, and compactness [1]. It was introduced by Shirasaki as a device that could achieve wavelength division multiplexing and dispersion compensating in optical communication systems [1–3]. Over the past decade, these researches have been further improved [4–7] and greatly extended to applications such as optical arbitrary waveform generation [8,9] and ultrafast optical pulse shaping [10,11]. Moreover, combining a VIPA with a diffraction grating which creates a two dimensional spectral dispersion leads to some other promising fields of applications including spectral encoded ultrafast imaging [12], molecular spectroscopy [13], spectral domain optical coherence tomography [14,15] and simultaneous endoscopic imaging and microsurgery [16,17]. Due to the superior optical performance and the potential value in application, researchers spare no effort to establish an accurate theoretical model to describe the spectral dispersion property of the VIPA. As a pioneer, Yang [18] presented an interfering distribution formula for the simple air-spaced VIPA by using the Fourier-transform, and found it was a function of diffraction angle. Vega *et al*. [19] proposed a dispersion equation via a qualitative analysis that the phase difference satisfies the constructive interference conditions. Xiao *et al* [20,21] derived a dispersion law by using the Fresnel diffraction analysis, which has been widely adopted in current reported applications. However, this dispersion law exists a subtle error and the effect of this error has been never analyzed. Mokhtari *et al* [22,23] formulated a more rigorous model for the VIPA and the output profile of a Gaussian beam array has been fully studied in a numerical method, while the most important dispersing performance of the VIPA is seldom considered. Recently, Gauthier [24] corrected a fundamental error existed in

#217519 - $15.00 USD Received 21 Jul 2014; revised 29 Nov 2014; accepted 30 Nov 2014; published 5 Jan 2015

Vega's model. Despite this correction combined with Weiner's [25] discussions about it provides a better understanding of the VIPA, the above mentioned theoretical models are not appropriate and accurate enough to describe the significant spectral dispersion of a general VIPA, especially for a solid VIPA.

In this paper, we present an effective and intuitional method to accurately describe the spectral dispersion of a general VIPA, as well as to overcome the drawbacks of the previous models. As a result of the diffraction divergence of the input Gaussian beam, it is considerably difficult to analyze the VIPA in real space. By taking advantage of the powerful diffraction theory of angular spectrum of plane waves, the input beam is decomposed into plane waves propagating with different directions (Sec. 2) which provides a fundamental precondition to study the extremely complicated diffraction propagation and interference behaviors of the output divergent beam series in angular space with a simple and straightforward geometrical approach. An intuitional spectral dispersion model of the VIPA is deduced in detail based on the interference theory and an exact analytical treatment of the previous model is also presented briefly (Sec. 3). By comparing the derived dispersion law with previous ones, the validity of the proposed model is validated theoretically. In addition, the effect of the optical aberrations to the dispersion law are analyzed (Sec. 4).

2. Fundamental principle

2.1 Working principle of VIPA

The VIPA resembles a windowed Fabry-Perot etalon in geometric structure, which mainly consists of two reflecting surfaces and an air-spaced or solid plane-parallel cavity as shown in Fig. 1. The back surface is coated with a partially reflective film (R_2≈95%), while the front surface is coated with a total reflective film (R_1≈100%) except for an antireflection coated area used as the entrance window, so that the energy efficiency of the input beam can be significantly enhanced [26,27]. The incident beam, which is typically a collimated fundamental mode (TEM_{00}) Gaussian beam, is weakly focused onto the back surface by a cylindrical lens and is coupled into the VIPA through the transparent window. Then, multiple back and forth reflections of the input beam at the two reflective films produce series of divergent beams transmitted from the back surface which satisfy the interference condition approximately. The interference of these beams not only leads to the output angles precisely varying with wavelength, but also leads to a narrow distribution of energy in angular space for any specific wavelength. Therefore, a hyperfine angular dispersion can be achieved. As the interference pattern is located at infinity, a focusing lens is usually used to observe the intensity distribution of this interference pattern at the back focal plane. From the above mentioned operating principle, the VIPA can be treated as a classical optical multiple beam interference device, more specifically, a Lummer–Gehrcke plate [28].

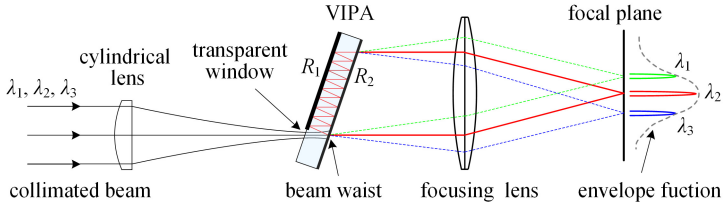

Fig. 1. Schematic geometry of the VIPA spectral disperser.

2.2. Angular spectrum representation of the input beam

As the input beam of the VIPA is generally only focused in one dimension (x direction) while the other dimension (y direction) still remains collimated, so the input beam is actually an

#217519 - $15.00 USD Received 21 Jul 2014; revised 29 Nov 2014; accepted 30 Nov 2014; published 5 Jan 2015

elliptical Gaussian beam located in *xy* plane. Then the amplitude distribution at beam waist plane ($z = 0$) will be given by:

$$E(x,y;0) = E_0 \exp\left(-\frac{x^2}{w_{0x}^2} - \frac{y^2}{w_{0y}^2}\right), \tag{1}$$

where E_0 is a constant amplitude, $w_{0x} = \lambda f_c /(\pi W)$ and $w_{0y} = W$ are the spot size of the Gaussian beam in direction of x and y, respectively, f_c is the focal length of the cylindrical lens, W is the beam radius of the collimated beam and λ is the wavelength in the propagation media.

By using angular spectrum of plane waves, the diffraction propagation of this Gaussian beam owing to its non-uniform amplitude distribution can be described as a superposition of plane waves propagating with direction cosines $\mathbf{e_k} = (\cos\alpha, \cos\beta, \cos\gamma)$, and the diffraction field (dropping the evanescent waves) follows the integral equation [29]:

$$E(x,y;z) = \int_{-\infty}^{+\infty}\int_{-\infty}^{+\infty} A(f_x, f_y)\exp\left[j2\pi\left(f_x x + f_y y + \sqrt{1-(\lambda f_x)^2 - (\lambda f_y)^2}\, z\right)\right] df_x df_y, \tag{2}$$

where the spatial frequencies are related to the direction cosines via $f_x = \cos\alpha/\lambda$ and $f_y = \cos\beta/\lambda$, respectively, $A(f_x, f_y)$ is defined as the angular spectrum of the field distribution $E(x, y; 0)$ and it is given by the following Fourier transform:

$$A(f_x, f_y) = \int_{-\infty}^{+\infty}\int_{-\infty}^{+\infty} E(x,y;0)\exp\left[-j2\pi\left(f_x x + f_y y\right)\right] dxdy. \tag{3}$$

Letting $\theta_x = \pi/2 - \alpha$ and $\theta_y = \pi/2 - \beta$, then $f_x = \cos\alpha/\lambda = \sin\theta_x/\lambda$ and $f_y = \cos\beta/\lambda = \sin\theta_y/\lambda$, where θ_x and θ_y corresponding to a definition of the field of view (FOV) are the output angle of diffraction. Substituting Eq. (1) into Eq. (3) yields the following expression that is the angular spectrum of the Gaussian beam [30]:

$$A(f_x, f_y) = A_0(\theta_x, \theta_y) = E_0' \exp\left[-\frac{k^2}{4}\left(w_{0x}^2 \sin^2\theta_x + w_{0y}^2 \sin^2\theta_y\right)\right], \tag{4}$$

where $E_0' = E_0\pi\, w_{0x}w_{0y}$ and $k = 2\pi/\lambda$. In arriving at Eq. (4), the well-known integral formula of $\int_{-\infty}^{+\infty}\exp(-\alpha x^2 + i\beta x) = \sqrt{\pi/\alpha}\exp[-\beta^2/(4\alpha)]$ is used twice independently, and the spatial frequencies $f_x = \sin\theta_x/\lambda$ and $f_y = \sin\theta_y/\lambda$ is used to simplify the result. According to Eq. (2), the diffraction of the input Gaussian beam of $E(x, y; z)$ can be investigated equivalently in angular space by using the plane wave components:

$$P(\theta_x, \theta_y; z) = A_0(\theta_x, \theta_y)\exp\left[jk\left(x\sin\theta_x + y\sin\theta_y + z\sqrt{1-\sin^2\theta_x - \sin^2\theta_y}\right)\right], \tag{5}$$

where $A_0(\theta_x, \theta_y)$ and $\mathbf{e_k} = [\sin\theta_x, \sin\theta_y, (1-\sin^2\theta_x - \sin^2\theta_y)^{1/2}]$ are treated as the amplitude and direction cosines of the plane wave in physical optics, respectively. Note that, by using Eq. (4) then Eq. (2) can be integrated in paraxial approximation to carry out the distinguished representation of a Gaussian beam [30].

3. Theoretical treatment of the VIPA

When analyzing a typical interference device, the ray-based geometry method is generally used to give a clear description of the phase difference which is the basis of studying interference phenomenon [28]. The angular spectrum representation of the input beam as given by Eq. (5) makes it possible to analyze the spectral dispersion of the VIPA in such a similar intuitional geometry method. But in this case, the rays should be considered as the

#217519 - $15.00 USD Received 21 Jul 2014; revised 29 Nov 2014; accepted 30 Nov 2014; published 5 Jan 2015

"diffracted rays", which corresponds to the geometrical theory of diffraction [31], instead of the ordinary rays of geometrical optics.

3.1. Theoretical derivation of the proposed model

Without loss of generality, we consider an oblique incidence of the plane wave described in Eq. (5) on a solid VIPA of thickness h (and of refractive index n') surrounded by a medium of refractive index n. When $n' = n = 1$, the following derivation will correspond to the air-spaced VIPA. If the symmetry plane of the VIPA is located in xz plane and the tilt angle of the VIPA in xz plane is denoted by φ, then the normal vector can be given by $\mathbf{e_n} = (-\sin\varphi, 0, \cos\varphi)$ as shown in Fig. 2(a). For the plane wave components with direction cosines $\mathbf{e_k} = [\sin\theta_x, \sin\theta_y, (1-\sin^2\theta_x - \sin^2\theta_y)^{1/2}]$, the incident angle Θ is given by:

$$\cos\Theta = \mathbf{e_n}\cdot\mathbf{e_k} = \cos\varphi\sqrt{1-\sin^2\theta_x-\sin^2\theta_y} - \sin\varphi\sin\theta_x. \tag{6}$$

The optical path differences (OPD) of the adjacent reflected waves can be simplified to $\Delta = 2n'h\cos\Theta'$ by using the geometric relationships shown in Fig. 2(a), and the corresponding phase difference $\delta = k\Delta$ is given by:

$$\delta = 2kh\left\{n^2\left[\cos\varphi\sqrt{1-\sin^2\theta_x-\sin^2\theta_y} - \sin\varphi\sin\theta_x\right]^2 + \left(n'^2-n^2\right)\right\}^{\frac{1}{2}}. \tag{7}$$

In arriving at Eq. (7), the Snell's Law $n'\sin\Theta' = n\sin\Theta$ and Eq. (6) have been utilized. As shown in Fig. 2(b), the optical path from O to P causes an additive phase δ_l which is given by:

$$\delta_l = k\left(d_z\cos\gamma + \frac{f}{\cos\gamma} - \frac{d_x}{\cos\eta}\sin\gamma\right), \tag{8}$$

where $\cos\gamma = (1-\sin^2\theta_x - \sin^2\theta_y)^{1/2}$, $\sin\eta = \tan\theta_y/\sin\gamma$, $\theta_x = \arctan(x_f/f)$, $\theta_y = \arctan(y_f/f)$, f is the focal length of the focusing lens, d_z is the distance from the beam waist to the lens and d_x is the displacement of the lens in the x direction.

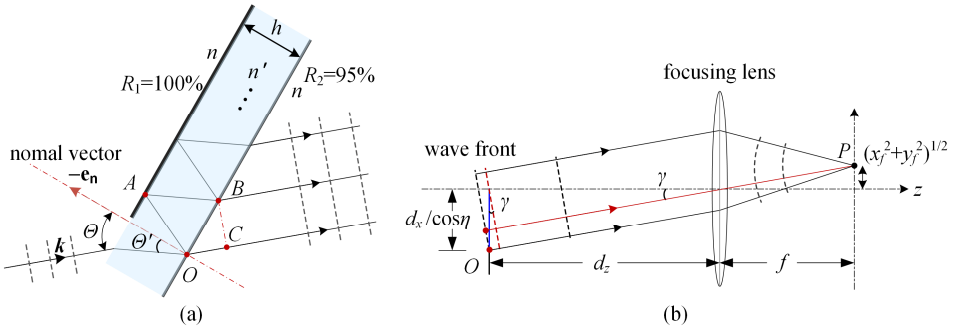

Fig. 2. (a) Sketch map of optical paths in the incident plane used to calculate the optical path differences (OPD) for the neighboring transmitted rays. The OPD is $\Delta = n'(OA + AB) - nOC = 2n'h\cos\Theta'$. (b) In the auxiliary plane, the optical path from the output plane to the back focal plane can be represented by the chief ray (red line) passing through the center of the lens. The incident plane and the auxiliary plane will be in the same cross-section if and only if $\theta_y = 0$.

As the beam enters the VIPA through the transparent window, we neglect the transmission coefficients of this window area, and let the amplitude reflection and transmission coefficients of the back surface be denoted by r_2 and t_2, respectively. According to the principle of multiple-beam interference [28], the complex amplitude of the transmitted waves

#217519 - $15.00 USD Received 21 Jul 2014; revised 29 Nov 2014; accepted 30 Nov 2014; published 5 Jan 2015

is given by $A_t = A_0 t_2 e^{j\delta_l} \sum_{m=0}^{M} (r_1 r_2 e^{j\delta})^m$, then the intensity distribution $I_t = A_t \cdot A_t^*$ will be written as:

$$I_t = A_0^{\,2} T_2 \frac{1+(R_1R_2)^M - 2(r_1r_2)^M \cos(M\delta)}{1+R_1R_2 - 2r_1r_2\cos\delta}. \tag{9}$$

Letting $R_1 = |r_1|^2 = 1$, $R_2 = |r_2|^2$, $T_2 = |t_2|^2 = 1- R_2$, and using the parameters defined in Eq. (1) and Eq. (4), through a proper simplification of Eq. (9), we obtain the intensity distribution of the interference pattern:

$$I_t = E_0'^2 \frac{(1-r_2^{\,2})(1-r_1^{M} r_2^{M})^2}{(1-r_1r_2)^2} \exp\left[-\frac{2f_c^{\,2}}{W}\sin^2\theta_x - \frac{2\pi^2 W^2}{\lambda^2}\sin^2\theta_y\right] \frac{1+F_M \sin^2(M\delta/2)}{1+F_1\sin^2(\delta/2)}, \tag{10}$$

where $F_i = 4r_1^{\,i} r_2^{\,i} (1- r_1^{\,i} r_2^{\,i})^{-2}$, $i = (1, M)$, $M \approx L/(2h\tan\varphi')$ is the number of reflection due to the finite length L of the VIPA and φ' is related to the tilt angle through $n'\sin\varphi' = n\sin\varphi$. In Eq. (10), the exponential term forms an envelope function while the remainder term results in the modulation of the intensity. Such an intensity modulation function is similar to the intensity distribution of the Lummer–Gehrcke plate [28]. The addition term $[F_M \sin^2(M\,\delta/2)] / [1 + F_1\sin^2(\delta/2)]$ broadens the line-width or the Full-width half-maximum (FWHM), but it does not affect the positions of the absolute maxima. Thus the intensity I_t will reach the maxima when the phase difference $\delta = 2m\pi$, where m is an integral.

So far, we achieve a rigorous description of the 2-D spectral dispersion for a VIPA, that is, the resonance conditions $\delta = 2m\pi$ or termed the dispersion law:

$$2kh\left\{n^2\left[\cos\varphi\sqrt{1-\sin^2\theta_x-\sin^2\theta_y} - \sin\varphi\sin\theta_x\right]^2 + \left(n'^2 - n^2\right)\right\}^{\frac{1}{2}} = 2m\pi. \tag{11}$$

Considering that the input Gaussian beam generally is collimated in y direction, so we neglect the divergence angle θ_y, which is restricted by the diffraction angles $\lambda/(\pi W)$ typically less than $0.5mrad$. If we let $\theta_y = 0$ and $\theta_x = \theta$ for simplification, the phase difference will be given by $\delta = 2n'k\,h\cos\Theta' = 2n'k\,h\cos(\varphi + \theta)'$. And the 2-D spectral dispersion law Eq. (11) will be transformed into a more useful 1-D spectral dispersion law:

$$2n'kh\cos(\varphi+\theta)' = 2kh\sqrt{n'^2 - n^2\sin^2(\varphi+\theta)} = 2m\pi, \tag{12}$$

by using the Snell's laws $n'\sin(\varphi + \theta)' = n'\sin(\varphi' + \theta') = n\sin(\varphi + \theta)$ and $n'\sin\varphi' = n\sin\varphi$.

Based on the spectral dispersion law Eq. (12), some useful relations can be obtained accordingly. The relation of the peak output wavelength λ and the output angle θ is given by:

$$(\Delta\lambda)_\theta = \lambda - \lambda_0 = \frac{2h}{m}\left[\sqrt{n'^2 - n^2\sin^2(\varphi+\theta)} - \sqrt{n'^2 - n^2\sin^2\varphi}\right], \tag{13}$$

where $m\lambda_0 = 2n'h\cos\varphi'$ and $m\lambda = 2n'k\,h\cos(\varphi + \theta)'$. The angular dispersion factor which represents the change in angle θ with the constructive interference wavelength is given by:

$$\frac{d\theta}{d\lambda} = -\frac{2\left[n'^2 - n^2\sin^2(\varphi+\theta)\right]}{n^2\lambda\sin 2(\varphi+\theta)}, \tag{14}$$

and the free spectral range (FSR) which represents the wavelength difference corresponding to a displacement of one order ($|\Delta\delta| = 2\pi$) is given by:

#217519 - $15.00 USD Received 21 Jul 2014; revised 29 Nov 2014; accepted 30 Nov 2014; published 5 Jan 2015

$$(\Delta\lambda)_{FSR} = \frac{\lambda}{m} = \frac{\lambda^2}{2h\sqrt{n'^2 - n^2\sin^2(\varphi+\theta)}}. \tag{15}$$

Another important relation is the spectral resolution $\Delta\lambda$ or spectral resolving power $R = \lambda/\Delta\lambda$. Letting the intensity modulation function $[1 + F_M \sin^2(M\,\delta/2)] / [1 + F_1\sin^2(\delta/2)]$ in Eq. (10) equal to 0.5, we will receive a transcendental equation about the FWHM ε_M [28] which can be solved approximately in numerical analysis methods. Then the spectral resolving power will be obtained by using the relation of$|\Delta\delta| = \varepsilon_M = 4\pi n'h(\Delta\lambda/\lambda^2)\cos(\varphi + \theta)' = 2\pi m(\Delta\lambda/\lambda)$ as follows:

$$R = \frac{\lambda}{\Delta\lambda} = \frac{2m\pi}{\varepsilon_M} = \frac{2kh\sqrt{n'^2 - n^2\sin^2(\varphi+\theta)}}{\varepsilon_M}. \tag{16}$$

For convenience consideration, the effect of F_M in Eq. (10) is usually dropped and the FWHM $\varepsilon_1 = 4.15(F_1)^{-1/2}$ will be given easily to replace ε_M.

In order to compare with previous works, the proposed dispersion law Eq. (12) can be rearranged as another equivalent form as follows

$$2kh\left[n'\cos\theta'/\cos\varphi' - n\tan\varphi'\sin(\varphi+\theta)\right] = 2m\pi. \tag{17}$$

In addition, by using the first order Taylor series expansions of the trigonometric functions of $\sin(\varphi' + \theta') = \sin\varphi' + \cos\varphi'\cdot\theta' + o(\theta')$ and $\sin(\varphi + \theta) = \sin\varphi + \cos\varphi\cdot\theta + o(\theta)$ together, we acquire the approximate relation $\theta' \cong \theta\cdot n\cos\varphi/(n'\cos\varphi')$. Substituting this relation into the second order Taylor series expansion of $\cos(\varphi' + \theta') = \cos\varphi' - \sin\varphi'\cdot\theta' - \cos\varphi'\cdot\theta'^2/2 + o(\theta'^2)$, then Eq. (12) is transformed into an approximate dispersion law:

$$kh\left[2n'\cos\varphi' - 2n\tan\varphi'\cos\varphi\cdot\theta - \frac{n^2\cos^2\varphi}{n'\cos\varphi'}\theta^2\right] = 2m\pi. \tag{18}$$

3.2. Accurate description of the previous virtual sources model

In previous model, the VIPA is regarded as a phase array consisting of virtual sources and the input beam is assumed to be a 1-D Gaussian beam. In this case, only θ_x is considered in Eq. (5) and the subscript is neglected ($\theta_x = \theta$) for simplicity. As show in Fig. 3(a), the space position distribution of the virtual sources is obtained through ideal imaging of the central ray of the focused beam. Not only the virtual beam waists themselves but also their transverse and longitudinal spacing are assumed to be identical.

According to Fig. 3(b), the transverse and longitudinal geometrical spacing of adjacent sources can be simplified to $\Delta x_0 = 2h\tan\varphi'\cos\varphi$ and $\Delta z_0 = 2hn_r\cos\varphi'$, respectively, where $n_r = n'/n$ represents the relative refractive index. These virtual sources are arranged in line at a certain direction determined by $\psi_1 = \arctan(\Delta x/\Delta z)$, while in previous analysis [1,32] an unreasonable conclusion is given that $\psi_1 = \varphi$, which is satisfied only for the specific condition $n_r = n'/n = 1$. The OPD of the adjacent diffracted rays with direction cosines $\mathbf{e_k} = (\sin\theta, 0, \cos\theta)$ can be simplified to $\Delta' = n\,(\Delta z_0\cos\theta - \Delta x_0\sin\theta)$. Taking advantage of the phase resonance conditions $\delta = k\Delta' = 2m\pi$, we obtain the accurate dispersion law of the previous model as follows:

$$2kh\left(n'\cos\varphi'\cos\theta - n\tan\varphi'\cos\varphi\sin\theta\right) = 2m\pi. \tag{19}$$

#217519 - $15.00 USD Received 21 Jul 2014; revised 29 Nov 2014; accepted 30 Nov 2014; published 5 Jan 2015

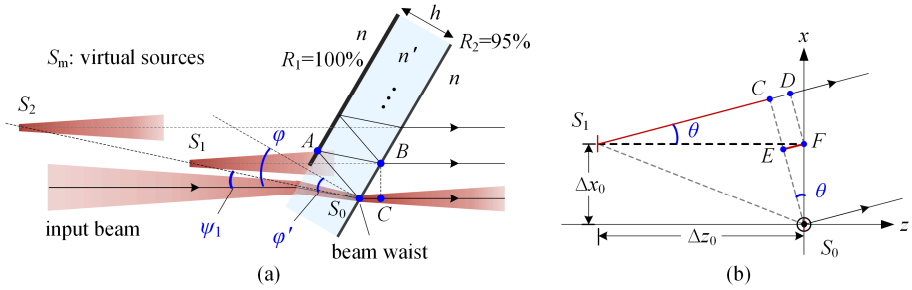

Fig. 3. Sectional view of a VIPA irradiated by the line-focused Gaussian beam for previous virtual sources model. (a) Considering the ideal reflection imaging of the beam waist, the geometrical spacing in the surrounding medium are $\Delta x_0 = BC = 2h\tan\varphi'\cos\varphi$ and $\Delta z_0 = (S_0A + AB)n'/n - S_0C = 2hn_r\cos\varphi'$. (b) For the diffracted rays with output angle of θ emitted from the adjacent sources, the OPD is describe as $\Delta' = nS_1C = n(S_1D - EF) = n(\Delta z_0\cos\theta - \Delta x_0\sin\theta)$.

Furthermore, by using the second order approximation $\sin\theta \cong \theta$ and $\cos\theta \cong 1 - \theta^2/2$, Eq. (19) is transformed into an approximate dispersion law:

$$kh\left[2n'\cos\varphi' - 2n\tan\varphi'\cos\varphi\cdot\theta - n'\cos\varphi'\cdot\theta^2\right] = 2m\pi, \tag{20}$$

which is identical to the dispersion law predicted by the paraxial wave theory [21]. Note that Xiao *et al.* [20] make an error [the Eq. (14)] while extending the theoretical derivation for the air-spaced VIPA to that of a solid VIPA, and this error is not found [the Eq. (4.33)] in Xiao's master thesis [21]. Therefore, Eq. (20) is the correct form of dispersion law deduced from Xiao's dispersion model.

4. Comparison and discussion

It is important to compare our results with previously proposed dispersion laws of the VIPA. As far as we know, there are only two detailed previous dispersion laws for the VIPA published by Vega *et al*. [19] and Xiao *et al*. [20], respectively. These two laws are all based on the assumption used in previous virtual sources model described at Section 3.2. Vega's dispersion law is given by [19]:

$$2kh\left[n'/\cos\varphi' - n\tan\varphi'\sin(\varphi+\theta)\right] = 2m\pi, \tag{21}$$

and Xiao's dispersion law which existing a subtle error in processes of simplification is given by [20]:

$$kh\left[2n'\cos\varphi' - 2n\tan\varphi'\cos\varphi\cdot\theta - \cos\varphi'\cdot\theta^2/n'\right] = 2m\pi. \tag{22}$$

Note that, in Eq. (21) and Eq. (22), the refractive index of the surrounding medium is assumed to be air (n = 1) in the following discussion and the descriptive symbols of the parameters have been changed to facilitate analytical comparison.

By comparing Eq. (21) and Eq. (17), we find that the difference is only caused by the coefficient of $\cos\theta'$ in the first term of Eq. (17). This is because in Vega's theoretical derivation only the central ray component of the input beam is considered, where $\theta' = 0$ so $\cos\theta' = 1$. The divergence of input beam after the beam waist can be interpreted as the inherent diffraction of the Gaussian beam. However, it is only considering the central ray component that results in the fundamental error found by Gauthier [24]. Actually, the diffraction propagation of the Gaussian beam can be equivalently described by using the plane wave components as shown in Eq. (5). Thus the result of our model Eq. (17) or the equivalent form Eq. (12) based on the plane wave method is obviously more effective than Vega's dispersion law. Since Xiao's dispersion law Eq. (22) based on the paraxial wave

#217519 - $15.00 USD Received 21 Jul 2014; revised 29 Nov 2014; accepted 30 Nov 2014; published 5 Jan 2015

theory is widely adopted when a VIPA is used, we focus our attention on it in the following comparison.

For the air-spaced VIPA ($n' = n = 1$, $\varphi' = \varphi$), Eq. (19) is perfectly equivalent to Eq. (12), that is, $2kh\cos(\varphi + \theta) = 2m\pi$. Meanwhile, Eq. (22) is reduced to $2kh[\cos\varphi(1 - \theta^2/2) - \theta\cdot\sin\varphi] = 2m\pi$, which is equivalent to Eq. (20). These two equivalent relations demonstrate that for the air-spaced VIPA the proposed model is completely equivalent to previous model, and Xiao's dispersion law Eq. (22) is an approximate representation of our dispersion law Eq. (12) in Fresnel approximation. So we can conclude that both our accurate law and Xiao's approximate law are appropriate to describe an air-spaced VIPA. Such a coincidence can be attributable to the assumption that the ideal reflection imaging of the Gaussian beam is perfectly acceptable in previous model. All of the virtual images are plane beam waist which is identical to that of the input Gaussian beam.

However, for a solid VIPA, the formation of the virtual images becomes extremely complicated because of the emergence of the optical aberrations generated by the refractions of the divergent beams at interfaces between two different media, including the transparent input area of the front surface and the whole back surface. In previous virtual sources model, such inherent optical aberrations were neglected and the assumption of ideal imaging of the input Gaussian beam was adopted. The virtual source array is obtained by only using the refraction and reflection imaging of the central ray as shown in Fig. 3(a) and Fig. 4(a), then the diffracted rays with wave-vector of $\boldsymbol{k}_\theta$ are assumed to be emitted from the these virtual source array. In other words, these diffracted rays except for the special treated central ray do not get through real refraction and reflection. In our proposed model, all rays with different wave-vectors are treated equally and they have got through real refraction and reflection independently while emitted from the back surface of the VIPA as shown in Fig. 4(a). In order to study the impact of the aberrations to the periodicity of the spatial distribution for the virtual sources, we consider the transverse and longitudinal geometrical spacing by using the relationship shown in Fig. 4(b), and define the variations of the geometrical spacing attribute to the optical aberrations to be $\Delta\xi = \Delta x_\theta - \Delta x_0$ and $\Delta\eta = \Delta z_\theta - \Delta z_0$. After a proper simplification, we have:

$$\Delta\xi = \frac{2h}{\sqrt{n_r^2 - \sin^2(\varphi+\theta)}}\left[\sin\varphi\cos(\varphi+\theta) - \left(n_r^2 - 1\right)\sin\theta\right] - 2h\tan\varphi'\cos\varphi, \quad (23)$$

and

$$\Delta\eta = \frac{2h}{\sqrt{n_r^2 - \sin^2(\varphi+\theta)}}\left[\cos\varphi\cos(\varphi+\theta) + \left(n_r^2 - 1\right)\cos\theta\right] - 2n_r h\cos\varphi'. \quad (24)$$

When $n_r = n'/n = 1$ ($\varphi' = \varphi$), $\Delta\xi = 0$ and $\Delta\eta = 0$, there is no aberrations existed, which corresponds to our analysis of the air-spaced VIPA. But for the solid VIPA, these aberrations result in the ideal planar beam waists vanished. As shown in Fig. 4(b), for every FOV with output angle θ the aberrations introduce a perturbation to the virtual source P depicted by using the central ray, so that the actual virtual source will be the point Q. The trajectory of the virtual source Q constitutes the first image $S_{1(\theta)}$ of the incident beam, the other images $S_{i(\theta)}$ can still be obtained likewise. So far, it is clear that when aberrations is considered the VIPA can still be treated similarly as a virtual phased array defined in previous model. But the corresponding spatial period changes from the previous constant of Δx_0 and Δz_0 [Fig. 3(a)] which depending on only the tilt angle φ to $\Delta x_\theta = \Delta\xi + \Delta x_0$ and $\Delta z_\theta = \Delta\eta + \Delta z_0$ which is a function of output angle θ.

The angular spectrum representation of the input beam allows us to effectively solve the ultimately useful phase difference of $\delta = k\Delta$ in a ray-based method as shown in Fig. 2(a) that the aberrations are considered indirectly. It is the above mentioned optical aberrations that

#217519 - $15.00 USD Received 21 Jul 2014; revised 29 Nov 2014; accepted 30 Nov 2014; published 5 Jan 2015

lead to the distinct difference in phase difference between dispersion laws Eq. (19) and Eq. (12) respectively given through previous model and the proposed model. In fact, such distinct difference in phase difference caused by optical aberrations impose effects not only on the dispersion law but also on the angular dispersion factor, the free spectral range (FSR) and the spectral resolving power, because they are all defined through the phase difference. Further, they are all in proportion to the phase difference. The above analysis demonstrates that our dispersion law Eq. (12) or its equivalent form Eq. (17) is the more reasonable and accurate dispersion law for a general VIPA because the intrinsic aberrations of refractions have been considered.

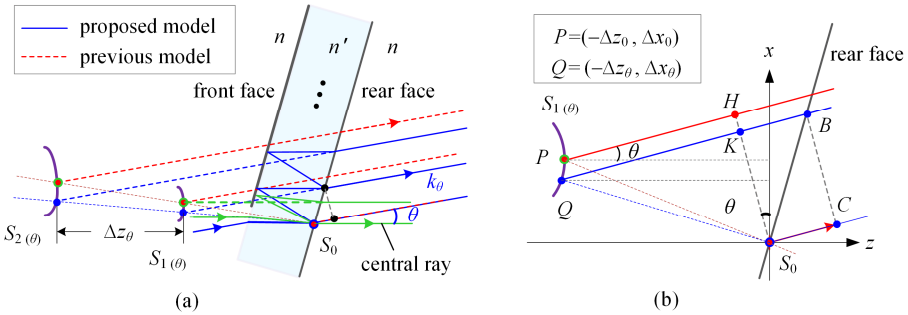

Fig. 4. Comparison of diffracted rays in a solid VIPA for the proposed model and the previous model. (a) In previous model, the virtual source array (red points) is depicted by using the refraction and reflection of central ray (green line), and other diffracted rays (red dashed line) are assumed to be emitted from these virtual sources. In proposed model, all rays are depicted by their real refraction and reflection (blue line). (b) Referring to Fig. 3(b), the OPD of the previous model can be describe as $\Delta' = nPH = n(\Delta z_0\cos\theta - \Delta x_0\sin\theta)$, and for the proposed model that is $\Delta = nQK = n(\Delta z_\theta\cos\theta - \Delta x_\theta\sin\theta) = 2n'kh\cos(\varphi + \theta)'$. With the help of another relation of $S_0K = EF + S_0D = BC$, we have $\Delta z_\theta\sin\theta + \Delta x_\theta\cos\theta = 2h\tan(\varphi + \theta)'\cos(\varphi + \theta)$. Then the spatial period Δz_θ and Δx_θ can be solved easily.

In Fig. 5, we illustrate the absolute deviations in phase difference as functions of the output angle and the tilt angle, which intuitively reflects the absolute error of the previous work as compared with the proposed model. Results in Fig. 5(a) show that absolute value of the deviations increase as the output angle increases when the tilt angle is fixed, and the results in Fig. 5(b) show that the deviations increase slowly as the tilt angle increases when the output angle is fixed except for that of Vega. The deviations between previous model Eq. (19) and the proposed model Eq. (12) depicts the effect of the optical aberrations given through Eq. (23) and Eq. (24). The deviations between Eq. (19) and Eq. (20), as well as Eq. (18) and Eq. (12) depict the effect of Taylor's series approximation. It is clearly shown in Fig. 5(a) that the extremely small deviations duo to Taylor's series approximation is insignificance when compared with the notable deviations duo to aberrations.

Another interesting result from Fig. 5(a) is that the correct form of Xiao's dispersion law Eq. (20) gives rise to a larger deviation than the original form of it Eq. (22) where an error exists compared with the proposed model that considering aberrations. In other words, although Eq. (22) is the incorrect result of the previous model, still it is an acceptable practical approximation law because the notable difference in phase difference caused by aberrations in the previous model is tremendously reduced by accident. Such a valuable coincidence in Eq. (22) can be easily explained in theory by comparing Eq. (18), Eq. (20) and Eq. (22). It can be seen that the discrepancies of these equations are only centralized on the quadratic terms related to output angle θ. Compared with the quadratic term of $n'\cos\varphi'\cdot\theta^2$ in Eq. (20), the term of $\cos\varphi'\cdot\theta^2/n'$ in Eq. (22) is more close to the term of $\cos^2\varphi\cdot\theta^2/(n'\cos\varphi')$ in Eq. (18) since $n' > n = 1$ and the practical tilt angle is usually small ($\varphi = 4°$). The accuracy and precision of Xiao's dispersion law Eq. (22) is in close proximity to the approximate

#217519 - $15.00 USD Received 21 Jul 2014; revised 29 Nov 2014; accepted 30 Nov 2014; published 5 Jan 2015

dispersion law Eq. (18) deduced by our proposed model as shown in Fig. 5(a), the deviation between them can be given by:

$$\Delta\delta = kh\left[\frac{\cos\varphi'}{n'} - \frac{n^2\cos^2\varphi}{n'\cos\varphi'}\right]\theta^2 + o(\theta^2). \tag{25}$$

Considering the deviations described by Eq. (25) is extremely small, so Eq. (22) can be treated as a useful empirical dispersion law because it neither a correct form of previous model nor a correct form of the proposed model. In addition, as we discussed above Xiao's dispersion law Eq. (22) is an acceptable practical approximation law and it has been verified by experiments [33]. Thus we can conclude that the proposed model and the corresponding dispersion law are appropriate to describe the VIPA accurately. Note that Eq. (25) can be used as the absolute correction value in phase difference for previous works which have adopted Xiao's dispersion law Eq. (22).

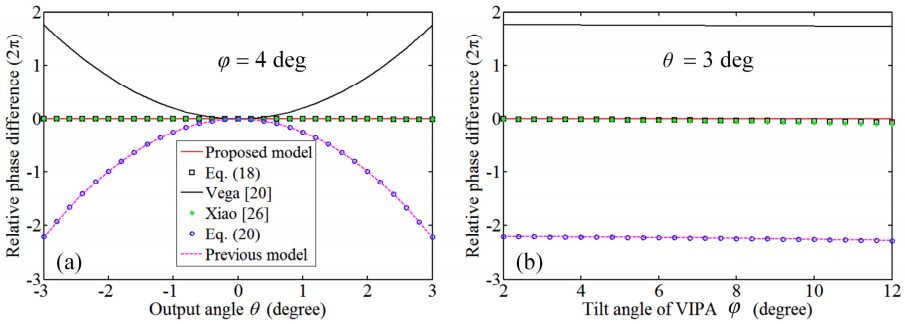

Fig. 5. Absolute deviations in phase difference for different dispersion laws, normalized by 2π, (a) as a function of output angle θ with tilt angle $\varphi = 4°$, and (b) as a function of the tilt angle φ with output angle $\theta = 3°$, while $n' = 1.5$, $n = 1.0$, $h = 1.5mm$ and $\lambda = 1.55\mu m$. The parameter values referenced from [33].

Finally, it is worth noting that in our analytical treatment the phase-shift caused by optical aberrations is considered, while the phase-shift related to the polarization of light is neglected because the effect of the polarization strongly depends on the specific characteristics of the reflective coatings [28]. It is quite difficult to obtain a general analytical expression for the polarization phase-shift, but we can qualitatively conclude that the polarization phase-shift is smaller than π which is much less than the deviations caused by optical aberrations depicted in Fig. 5. A numerical analysis of the polarization for the VIPA refers to the work of Mokhtari *et al* [23]. Furthermore, it is particularly meaningful to point out that the analytical spectral dispersion law Eq. (12) derived from our plane wave method is a general accurate dispersion law for the VIPA, which is both valid whether the paraxial approximation is satisfied or not. This means that through a proper reshaping of the input beam to enlarge the divergence angle we may get rid of the restrictions of the paraxial approximation used in previous works. In this case, the diffraction envelope function in Eq. (10) will be changed but the dispersion law of Eq. (12) remains unchanged. In addition, the distance (d_z) from the output plane of the VIPA to the front focal plane of the focusing lens can be changed arbitrarily as the specific needing of optimization, and it is unnecessary to keep this distance equal to the focal length of the lens because d_z has no effect on the interference intensity distribution [described in Eq. (10)] observed at the back focal plane.

5. Conclusion

We have proposed an analytical spectral dispersion model for the VIPA based on the theory of the multiple-beam interference. By using the angular spectrum approach, the diffraction

#217519 - $15.00 USD Received 21 Jul 2014; revised 29 Nov 2014; accepted 30 Nov 2014; published 5 Jan 2015

propagation and multiple reflections of the input beam for a general VIPA are studied. A clear theoretical treatment of the VIPA is given and a rigorous analytical spectral dispersion law is obtained. It is demonstrated in a comparison with the previous reported laws that the proposed law is more reasonable to describe the spectral dispersion of a general VIPA because the optical aberration is considered. In addition, our model provides a clear physical interpretation of the phase-matching condition, which is conducive to the understanding of the spectral dispersion property of the VIPA. Our analytical treatment and results are useful for the design and optimization of the devices and optical systems based on VIPA spectral dispersers as mentioned in the introduction.

Acknowledgments

The authors would like to acknowledge the financial supports from the National Major Scientific Instruments and Equipment Development Project (NO. 2013YQ14051702) and the Project of Jilin Province Science and Technology Hall (NO. 20140204030GX).